Chemico-Biological Interactions 316 (2020) 108933

Contents lists available at ScienceDirect

Chemico-Biological Interactions

journal homepage: www.elsevier.com/locate/chembioint

Effects of inflammation on irinotecan pharmacokinetics and development of a best-fit PK model

Pavan Kumar Chityala, Lei Wu, Diana S-L Chow, Romi Ghose*

Department of Pharmacological and Pharmaceutical Sciences, College of Pharmacy, University of Houston, 4800 Calhoun Rd, Houston, TX, 77004, USA

ARTICLE INFO

Keywords:
Irinotecan
CPT-11
SN-38
Inflammation
Pharmacokinetics
Drug metabolizing enzymes
Pharmacokinetic modeling
Phoenix WinNonlin
Phoenix NLME

ABSTRACT

Irinotecan is a chemotherapeutic drug used in the treatment of advanced colorectal cancer and elevated blood concentrations of its active metabolite, SN-38 leads to increased gastrointestinal (GI) toxicity and diarrhea in patients. In this study, we investigated the effects of inflammation on the pharmacokinetics (PK) of irinotecan (CPT-11) and its active metabolite, SN-38. Mice were i.p.-injected with either saline or lipopolysaccharide (LPS) to induce inflammation. After 16 h, irinotecan was administered orally. Blood was collected from the tail vein of mice from 0 to 24 h after dosing. Concentrations of irinotecan, SN-38 and SN-38G were analyzed using LC-MS/MS. The AUC, C_{max}, and t_{max} were derived using WinNonlin® 5.2. A PK model was developed using Phoenix NLME® to describe the PK of irinotecan and SN-38 during inflammation. Results indicated a significant increase in the blood concentrations of irinotecan and SN-38 in mice during inflammation. The AUC of irinotecan and SN-38 in LPS group were 2.6 and 2-folds, respectively, of those in control saline-treated mice. The C_{max} of irinotecan and SN-38 in LPS treated mice were 2.4 and 2.3-folds of those in saline-treated mice. The PK model was successfully developed and validated. The best-fit plots of individual PK analysis showed a good correlation between observed and predicted concentrations of irinotecan and SN-38. Together, this study reveals that SN-38 concentrations are elevated during inflammation, which may increase the GI toxicity and diarrhea in patients who receive irinotecan; and the developed PK model can quantitatively describe the PK of irinotecan and SN-38 during inflammation.

1. Introduction

Irinotecan (CPT-11) is a first-line chemotherapeutic drug for advanced colorectal cancer [1,2]. Irinotecan is a pro-drug to the active metabolite, 7-ethyl-10-hydroxycamptothecin (SN-38), which is approximately 100 to 1000-fold more cytotoxic than the parent compound [3–6]. SN-38 shows its anticancer activity by inhibiting the topoisomerase-I enzyme [7–9], which is involved in DNA replication. The SN-38 metabolite is formed from irinotecan by the carboxylesterase enzyme and is further conjugated to an inactive glucuronide (SN-38G) metabolite by the UGT1A1 enzyme [10]. Enterohepatic recycling (EHR) occurs when SN-38G is deconjugated back to SN-38 by bacterial β-glucuronidases produced in the intestine, followed by reabsorption of SN-38 [11]. The CYP3A4 enzyme metabolizes irinotecan to inactive, non-toxic metabolites APC and NPC [12–15].

Irinotecan-induced gastrointestinal (GI) toxicity has been extensively studied [16–19], and the major dose-limiting toxicity is diarrhea. Generally, diarrhea caused by irinotecan is the result of increased exposure of intestinal epithelium to the active metabolite, SN-38. Delayed diarrhea is observed in up to 87% of patients, with 30–40% experiencing severe diarrhea (grade 3 or 4) [20,21]. Due to the severe diarrhea caused by irinotecan, the dose given to patients is reduced, which limits the use of irinotecan as a chemotherapeutic agent, resulting in limited efficacy of drug in approximately 40% patients [23].

Well-established studies have shown that during inflammation, the expression and activities of many drug-metabolizing enzymes (DMEs) and transporters were significantly altered [24–31]; the enzymes involved in irinotecan metabolism are primarily down-regulated. Specifically, cyp3a11 RNA levels are reduced in mouse liver by lipopolysaccharide (LPS), or lipoteichoic acid (LTA), which are components of gram-negative and gram-positive bacteria, respectively [24,30]. Treatment with LPS was shown to decrease the expression and hydrolytic activity of human carboxylesterase 1 and 2 (HCE 1 and HCE 2) *in vitro* and *in vivo* [32]. Hepatic expression of the phase-II enzyme, ugt1a1 was also reduced by LPS treatment for 16 h in mice [33]. Therefore, it is likely that irinotecan metabolism and PK will be altered during infection or inflammation due to the reduced expression and activity of several key enzymes.

* Corresponding author. 4849 Calhoun Rd, Room 3041, College of Pharmacy, University of Houston Houston, TX, 77204, USA.
E-mail address: rghose@uh.edu (R. Ghose).

https://doi.org/10.1016/j.cbi.2019.108933
Received 31 August 2019; Received in revised form 29 November 2019; Accepted 19 December 2019
Available online 20 December 2019

A strong correlation exists in the literature between the incidence of irinotecan-induced diarrhea and the area under the plasma concentration versus time curve (AUC) of its active metabolite, SN-38. For instance, Sasaki et al. showed that the episodes of diarrhea had a better correlation with the AUC of SN-38 than that of irinotecan [17], and with multivariate analysis, concluded that the AUC of SN-38 is a significant variable for the incidence of diarrhea [17]. Similarly, few other studies also showed a significant correlation with the blood concentrations of SN-38 and development of diarrhea [18,19]. Therefore, in the present study, we have investigated the PK of irinotecan and its metabolites, SN-38 and SN-38G in mice treated with LPS. We determined the AUC, C_{max}, and t_{max} for irinotecan, SN-38, and SN-38G. In addition, we developed a PK model using Phoenix NLME® to predict irinotecan and SN-38 concentrations during inflammation. Together, this study aims to identify and characterize the effects of inflammation on the PK of irinotecan and SN-38.

2. Materials & methods

2.1. Chemicals

Camptothecin (CPT; internal standard) was purchased from Millipore Sigma (St Louis, MO). Irinotecan hydrochloride was purchased from Martin Surgical Supply (item no: 4434-11, Houston, TX). SN-38 was purchased from Cayman Chemical (item no: 15632, Ann Arbor, MI). SN-38G was synthesized in Dr. Ming Hu's lab at the University of Houston, Houston, TX. All solvents used for chromatographic analysis were of LC-MS grade and purchased from VWR International, LLC (Suwanee, GA, USA). Unless specified, all other chemicals and reagents were purchased from Millipore Sigma (St. Louis, MO).

2.2. Animals

Male 5-weeks old C57BL6J mice were purchased from Jackson Laboratory (Ban Harbor, ME). The animals were kept in an environmentally controlled room (temperature 25 ± 2 °C, 12 h dark-light cycle, humidity 50 ± 5%) for at least 1 week before performing any experiments. The mice were on a regular diet ad libitum throughout the animal study. All the protocols followed for animal care and use were approved by the Institutional Animal Care and Use Committee (IACUC) at the University of Houston.

2.3. Study design and drug treatments

Mice (n = 5) were injected with saline or LPS (2 mg/kg) intraperitoneally (i.p.) and after 16 h, a single dose of 10 mg/kg irinotecan hydrochloride was given via oral route of administration. Blood samples of approximately 20 μl were collected from the tail vein at 0 h (pre-dose) and 0.25, 0.5, 1, 2, 4, 6, 10, and 24 h post the irinotecan administration. After the 24 h sample, mouse livers were isolated, flash-frozen in liquid nitrogen and stored at −80 °C until further use.

2.4. Sample preparation, LC-MS/MS quantification, and PK studies

For LC-MS analysis, the frozen samples were thawed and prepared by mixing approximately 10 μl of blood samples with 10 μl of PBS. To this mixture, 200 μl of 50% of acetonitrile (ACN) containing 5 μM camptothecin (internal standard) was added as an extracting solvent. Samples were vortexed for 30 s and centrifuged for 15 min at 18,000 × *g*. After the centrifugation, one-hundred and eighty (180) μl of supernatants were collected and allowed to dry under a gentle stream of air at room temperature. The air-dried samples were then reconstituted with 100 μl of 50% acetonitrile and samples were centrifuged for 10 min at 8000 × *g*. Eighty (80) μl of the supernatant was transferred to vials and 10 μl was injected into LC-MS/MS for analysis of irinotecan, SN-38, and SN-38G.

To analyze irinotecan and metabolite concentrations, an API 5500 QTRAP triple quadrupole mass spectrophotometer (AB Sciex, USA) equipped with a Turbospray TM source was used by multiple reaction monitoring (MRM) method operated in a positive ion mode, with minor modifications to the method conditions as previously described [36]. A UPLC system, Waters Acquity™ with a diode-arrayed detector (DAD) was used. The UPLC conditions were as follows: column, Acquity UPLC BEH C18 column (50 mm × 2.1 mm I.D., 1.7 μM, Waters, Milford, MA, USA); mobile phase A - 0.1% formic acid and mobile phase B - 100% acetonitrile performed in a gradient from 0 to 4.5 min. The flow rate and sample injection volume were 0.4 ml/min and 10 μL, respectively. The following *m/z* transitions were selected: *m/z* 587.1 → 124.1 for irinotecan, *m/z* 393.1 → 349.1 for SN-38 *m/z* 569.5 → 393.1 for SN-38G and *m/z* 349.0 → 305.1 for CPT. The selection of the fragment ions depended on the highest intensity of the fragment. The data collected was analyzed with Analyst 1.4.2 software (AB Sciex, USA).

2.5. Determination of AUC, C_{max}, t_{max} by WinNonlin

The AUC, C_{max}, and t_{max} values for saline and LPS groups were determined using compartmental analysis by WinNonlin 5.2 (Pharsight Corporation, Mountain View, CA, USA). AUC values are expressed in 'ng.h/ml'. C_{max} and t_{max} values are reported in 'ng/ml' and 'h', respectively.

2.6. PK Co-modeling of irinotecan and SN-38

The PK model was developed based on the observed concentration vs. time data for irinotecan and SN-38 in mouse blood samples in saline and LPS groups (n = 5 per group). Initial estimates of individual compartmental PK parameters were derived using Phoenix NLME (nonlinear mixed effect) (Pharsight Corp., Mountainview, CA, USA). Concentrations of irinotecan and SN-38 were fitted simultaneously. Model structures were developed based on actual dosing, sampling times and mass balance equations. Model discrimination on data was performed using Phoenix, by minimizing the Akaike Information Criterion (AIC) and by the comparison of the quality of plot fits, such as using a large amount of observed data vs. fitted data, weighted residual vs. fitted data, and weighted residual vs. time.

Different compartmental PK models were tested to describe the irinotecan and SN-38 concentrations in different compartments. Enterohepatic recycling (EHR) compartment was included in the PK model, with a linear transfer of irinotecan to EHR compartment and nonlinear transfer of SN-38 to EHR compartment. The model was developed to establish the relationship of irinotecan and SN-38 to EHR compartment. We omitted SN-38G data in the model in order to better describe the irinotecan and SN-38 data with high reliability and without much complexity.

Individual estimates of PK parameters were assumed to follow a log-normal distribution. Therefore, an exponential distribution model was used to account for inter-subject variability (IIV) as follows:

$$P_i = P \cdot exp(\eta_i)$$

where P_i is the individual parameter estimate for individual i, P is the typical population parameter estimate, and η_i was assumed to be distributed N (0, ω2), with a mean of 0 and variance of ω2. Only significant IIVs in PK parameters were retained.

Residual unexplained variability was implemented as either a proportional or combined error model:

$$C_{observed,ij} = C_{pred,ij} \times (1 + \varepsilon_{p,ij}) + \varepsilon_{a,ij}$$

where $C_{observed,ij}$ represents the observed concentration for individual i and observation j, $C_{pred,ij}$ represents the individual predicted concentration. $\varepsilon_{p,ij}$ and $\varepsilon_{a,\ ij}$ represent the proportional and additive errors

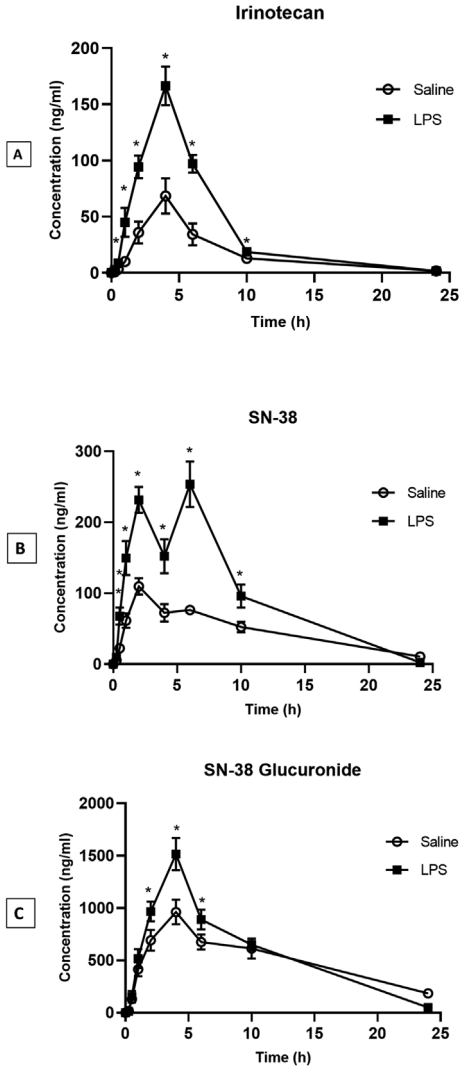

Fig. 1. Observed blood concentration-time profiles of irinotecan **(A)**, its pharmacologically active metabolite, SN-38 **(B)**, and inactive glucuronic acid conjugate SN-38G **(C)** after a single dose oral administration of 10 mg/kg irinotecan.

distributed following N (0, σ2), with a mean of 0 and variance of σ2. Selection of an appropriate residual error model was based on the likelihood ratio test and the inspection of the goodness-of-fit plots.

2.7. Statistical analysis

Data are expressed as mean ± standard deviation for all the experiments. Statistical analysis was performed using *t*-test to compare the significance between saline and LPS groups. GraphPad Prism 8.0 software was used for the analysis and P-value of < 0.05 was considered as statistically significant.

3. Results

3.1. PK of irinotecan and metabolites

The observed concentration-time profiles for irinotecan, SN-38, and SN-38G obtained from 0 to 24 h after irinotecan administration in saline or LPS mice groups are shown in Fig. 1. When compared to the saline group, the blood concentrations of irinotecan and SN-38 were significantly higher in the LPS group from 0.25 to 10 h. On the other hand, the blood concentrations of SN-38G in LPS group were significantly elevated only at 2, 4, and 6 h. Interestingly, the SN-38 concentration-time profile showed a significant second peak at 6 h in the LPS group, while the second peak was much lower in the saline group. This suggests that inflammation may increase the EHR and reabsorption of SN-38 in the LPS group.

The $AUC_{0\text{-}24}$, C_{max}, and t_{max} were determined by WinNonlin 5.2 (Table 1). The AUC, C_{max}, and t_{max} values for irinotecan, SN-38, and SN-38G were derived based on their concentrations and the estimates of parameters from the established compartmental model. The compartmental analysis showed that the AUC of irinotecan (994.2 ± 34.7 ng h/ml) in the LPS group with inflammation was approximately 2.6-fold of that in the saline group (381.4 ± 60.1 ng h/ml). In addition, the C_{max} of irinotecan in the LPS group (144.3 ± 10.1 ng/ml) was 2.4-fold of those in the saline group (59.6 ± 12.8 ng/ml). Similarly, the AUC of SN-38 in LPS group (2364.3 ± 275.1 ng h/ml) was significantly higher with a 2-fold increase compared to that in the saline group (1194.4 ± 139.2 ng h/ml), and the C_{max} of SN-38 in the LPS group (226.5 ± 8.7 ng/ml) was 2.3-fold higher to that of the saline group (96.6 ± 6.1 ng/ml). On the other hand, no significant difference was observed in the AUC or C_{max} of SN-38G between saline and LPS groups. The AUCs of SN-38G in saline and LPS groups were 13,895.4 ± 1795.4 ng h/ml and 12,428.5 ± 660.4 ng h/ml, respectively. The t_{max} was not apparently altered with inflammation.

3.2. PK model development and validation

A best-fit model to describe the PK of irinotecan and SN-38 in blood was developed. The model consisted of one compartment each for irinotecan and SN-38 connected with a rate constant K12 of the conversion process, and a third compartment connected with irinotecan and SN-38 for EHR. The final model structure is presented in Fig. 2. The model was described by the mass balance equations listed below:

A1 for irinotecan = - (A1 *K1e) + (Aa * Ka)- (A1 *k12)- (A1 *K13- A3 *K31)

A2 for SN-38= (A1 *k12)- (A2 *K2e) - (V_{max} * SN-38/(SN-38 + Km))

A3 = (V_{max} * SN-38/(SN-38 + Km)) + (A1 *K13- A3 *K31)

$A_{irinotecan}$ = (A1 *K1e)

Aa = - (Aa * Ka)

$A_{sn\text{-}38}$ = (A2 *K2e)

The results indicate that the inclusion of non-linear PK transferring from SN-38 to EHR compartment significantly improved the model

Table 1
AUC, C_{max}, t_{max} of irinotecan, SN-38, SN-38G in saline and LPS groups, derived using WinNonlin 5.2.

	Irinotecan		SN-38		SN-38G	
	Saline	LPS	Saline	LPS	Saline	LPS
AUC (ng.h/ml)	381.4 ± 60.1	994.2 ± 34.7*	1194.4 ± 139.2	2364.3 ± 275.1*	13895.4 ± 1795.4	12428.5 ± 660.4
C_{max} (ng/ml)	59.6 ± 12.8	144.3 ± 10.1*	96.6 ± 6.1	226.5 ± 8.7*	857.7 ± 84.0	1289 ± 68.0
t_{max} (h)	3.4 ± 0.2	3.3 ± 0.2	2.4 ± 0.3	3.5 ± 0.4	3.8 ± 0.2	3.7 ± 0.3

Note: * indicates a statistical significance ($p < 0.05$).

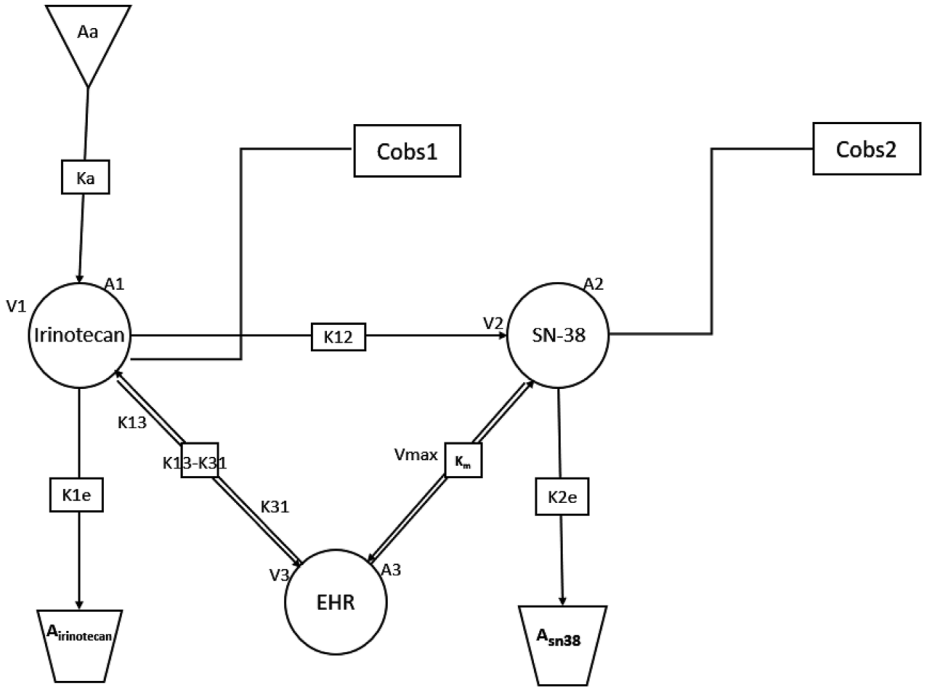

Fig. 2. The model structure and parameters of the best fit PK Model of irinotecan and SN-38 with EHR
Ka: absorption rate constant, irinotecan compartment
K12: rate constant, irinotecan to SN-38
K1e: elimination rate constant, irinotecan compartment
K2e: elimination rate constant, SN-38 compartment
V_{max}: maximum rate, the saturable process between SN-38 and EHR compartment
K_m: the Michaelis Menten constant, the saturable process between SN-38 and EHR compartment
K13: rate constant, irinotecan to EHR compartment
V1: volume distribution in irinotecan compartment
V2: volume distribution in SN-38 compartment
Cobs1: concentrations observed for compartment 1 (irinotecan)
Cobs2: concentrations observed for compartment 2 (SN-38)
$A_{irinotecan}$: elimination phase of irinotecan
A_{sn38}: elimination phase of SN-38.

fitting.

Based on the best-fit PK model developed, individual PK analysis of irinotecan and SN-38 was performed using observed blood concentrations-time data of irinotecan and SN-38 in each mouse to derive the PK parameters of individual mice. The average values of each PK parameter for saline and LPS groups are reported and compared with Student's t-test in Table 2. The model also revealed a nonlinear PK process of SN-38 transferring to EHR compartment with V_{max} and K_m characterized. The inflammation resulted in a significant reduction of conversion rate (K12) of irinotecan to SN-38 and increased Km in EHR of SN-38.

Predicted individual PK profiles of irinotecan and SN-38 were simulated using the best-fit model and derived PK parameters. (Fig. 3a). Good correlations were observed between observed and predicted values of irinotecan and SN-38 in all mice (Fig. 3b).

Fig. 4 represents the diagnostic plots of individual weighted residuals (IWRES) versus individual predicted concentration (IPRED) profiles, in which, all weighted residuals fall within the narrow range of −2 to 2 of IWRES and distributed around the line of 0 on Y-axis for irinotecan and SN-38 compartments. The diagnostic plots of IWRES versus time (TAD) profiles in irinotecan and SN-38 compartments are presented in Fig. 5. These diagnostic plots from PK modeling indicated that the best fit model of irinotecan and SN-38 could simultaneously describe the blood concentration profiles of irinotecan and SN-38, with reliability and stability for all mice in the saline and LPS treated groups.

Table 2
PK parameters of irinotecan and SN-38 in saline and LPS groups predicted individually from developed PK model.

Parameter	Unit	Saline Group	LPS Group	p-value
K12	1/h	0.53 ± 0.08	0.36 ± 0.11*	0.023
Km	ng/mL	183.13 ± 71.12	610.96 ± 186.91*	0.004
V_{max}	mg/h	2.49 ± 0.90	2.96 ± 1.07	0.232
Ka	1/h	0.17 ± 0.03	0.19 ± 0.07	0.478
V1	L	40.85 ± 8.90	21.16 ± 9.47	0.129
K1e	1/h	0.23 ± 0.31	0.03 ± 0.05	0.246
V2	L	0.006 ± 0.004	0.005 ± 0.003	0.314
K2e	1/h	0.11 ± 0.06	0.10 ± 0.15	0.428
K13	1/h	0.04 ± 0.07	0.03 ± 0.02	0.222
K31	1/h	0.60 ± 0.84	0.0003 ± 0.0004	0.091

Note: * indicates a statistical significance ($p < 0.05$).

4. Discussion

To our knowledge, this is the first study that describes the PK of irinotecan, SN-38, and SN-38G during inflammation. In this study, we (1) investigated the effects of inflammation on the PK of irinotecan, SN-38, and SN-38G, and (2) developed a co-model to simultaneously describe the PK of irinotecan and SN-38 during inflammation with parameters characterized. It is well known that during inflammation, the expression and activity of drug-metabolizing enzymes (DMEs) and transporters are reduced, mainly due to transcriptional suppression or as a result of post-translational protein modification, induced by mediators such as pro-inflammatory cytokines (IL-6, TNF-α, IL-1β) [25,37–42]. The reduction in the expression and activity significantly alters drug metabolism, pharmacokinetics, and pharmacodynamics (PK/PD) of drugs, and therefore poses a risk for toxicity and drug-drug interactions [27,43–46]. As reported in our results, the AUC of irinotecan and SN-38 were significantly elevated in mice after LPS treatment, with an increase of 2.6-folds for irinotecan and 2-folds for SN-38 when compared with the saline group. The significant increase in irinotecan concentrations could be due to the downregulation of carboxylesterase enzyme expression during inflammation, as reported by Mao et al. (2011) [32], and confirmed with the decreased conversion rate constant, K12 in our developed PK model. The downregulation of CEs expression and activity could result in reduced phase-I metabolism of irinotecan, which converts the parent compound to SN-38.

As it is known that irinotecan chemotherapy causes severe diarrhea in patients, the 2-fold elevation of SN-38 concentrations during inflammation presents a higher risk of toxicity that may warrant dosage modifications in these patients who receive irinotecan. As ugt1a1 is known to be down-regulated during inflammaton [33,47,48], a possible mechanism for the elevation of SN-38 during inflammation could be the reduction in the expression and activity of ugt1a1.

Furthermore, the reduced expression and activity of UGT1A1 during inflammation may have contributed to the reduction in phase-II metabolism and conversion of SN-38 to inactive SN-38G, which results in a decreased clearance and increased accumulation of SN-38. This

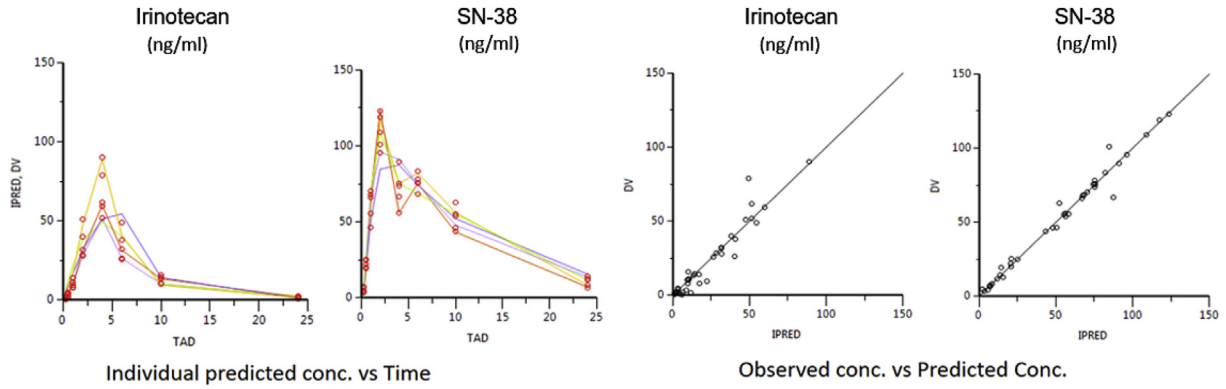

Fig. 3. Plots of individual predicted concentration (IPRED) vs time after dose (TAD) **(3a)** and observed concentration vs predicted concentration **(3b)** for irinotecan and SN-38.

observation suggests that patients who receive irinotecan during inflammation may have an increased risk of experiencing severe, life-threatening diarrhea due to the significant elevation of SN-38 concentrations. On the other hand, there is limited evidence present on the regulation of intestinal β-glucuronidase enzyme expression and activity during inflammation *in vivo*. A recent study shows that LPS increases β-glucuronidase activity in liver cells [49]. Based on the elevated concentrations of SN-38 and the observation of a second peak in the PK profile of SN-38, a possible mechanism could also be the increase in the activity of β-glucuronidase enzyme during inflammation, which may have increased the reconversion of inactive SN-38G to active SN-38. This is consistent with our observation that SN-38G blood concentrations were unchanged by LPS treatment. Together, the downregulation of UGT1A1 and upregulation of β-glucuronidase enzymes might have played significant roles in the elevated blood SN-38 concentrations and AUC during inflammation.

As we observed a significant increase in SN-38 concentrations and AUC in mice with LPS treatment, we aimed to develop a PK model that can describe the correlation between irinotecan and SN-38 concentrations during inflammation. To date, a number of pharmacokinetic models were developed and published in various studies to describe irinotecan and SN-38 PK [10,17,50–53]. However, the co-modeling approach used in this study is novel, as for the first time, the effect of inflammation is incorporated in the PK model building. The proposed and validated PK model in this study can be used to accurately predict the plasma concentration of irinotecan and SN-38. The best fit structural model consisted of compartments for irinotecan, SN-38 and EHR compartment connected with different rate constants. The model fitting exercises revealed nonlinear PK process of SN-38 transferring between EHR compartment with V_{max} and K_m. After the inclusion of non-linear PK for SN-38 and EHR compartments, the model was developed and model discrimination was performed on data using Phoenix, by minimizing the Akaike Information Criteria (AIC) and by comparison of the quality of fit plots. With the best fit model of irinotecan and SN-38, good correlations between observed and predicted concentrations were obtained in irinotecan and SN-38 compartments. The PK parameters described in the model were derived from 10 mice (5 mice per group). The standard deviation of PK parameter estimates (Table 2) revealed a small variation among 5 mice in each group, which reflected in the stability of the model. The rate constant K12 was significantly decreased, indicating that the conversion of irinotecan to SN-38 is reduced during inflammation. The K_m was significantly increased in the LPS group, indicating that the affinity of SN-38 to transporters involved in the recycling process was decreased during inflammation. Moreover, it is apparent with our model that during inflammation, the EHR increased with a higher Km and resulted in a significant second peak in the SN-38 profile.

The diagnostic plots from the developed model indicate that the best-fit PK model of irinotecan and SN-38 was highly stable to simultaneously describe the PK of irinotecan and SN-38 data with reliability in mice during inflammation. In addition to the effects of inflammation, the model also allowed us to successfully evaluate the effects of enterohepatic recycling in describing the PK of irinotecan and SN-38. The therapeutic implication of our research is that patients with inflammation should receive lower doses of irinotecan to achieve the same exposure as normal patients without inflammation. Using the developed model, we documented the impact of inflammation on irinotecan PK quantitatively, which is useful to rationally adjust the dose of irinotecan to minimize the toxicity.

A limitation of this study is that only 10 mice were employed. A large sample size would have enhanced the predictive performance of our modeling results. Further studies focusing on irinotecan metabolism

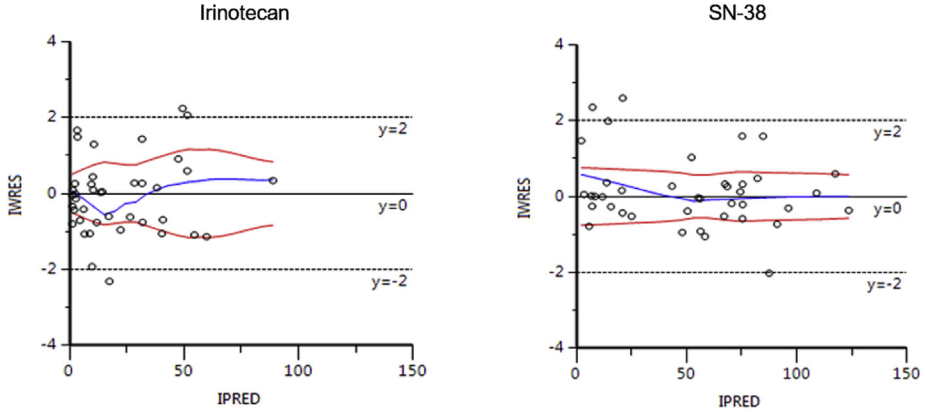

Fig. 4. Diagnostic plots of individual weighted residual (IWRES) vs individual predicted concentration (IPRED) for irinotecan and SN-38.

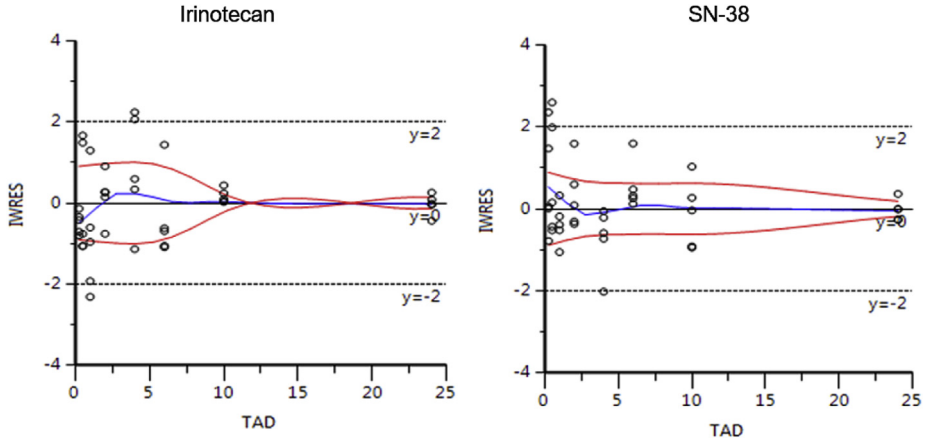

Fig. 5. Diagnostic plots of individual weighted residual (IWRES) vs time after dose (TAD) for irinotecan and SN-38.

should be conducted and the mechanism of EHR elimination should be clearly demonstrated in the future.

5. Conclusion

The present study investigated the effects of inflammation on the PK of irinotecan and its metabolites SN-38, and SN-38G. Our research showed that during inflammation, the concentrations of irinotecan and SN-38 were elevated, likely because inflammation altered the expression and activities of phase-I and phase-II enzymes that are involved in irinotecan metabolism. This study also found that the AUC and C_{max} of irinotecan and SN-38 were significantly higher in mice with inflammation, which indicates that the patients with inflammation may experience severe toxicity in the form of diarrhea due to the increased exposure to SN-38. This research suggests a need for the adjustment of irinotecan dose in patients during inflammation. We further developed a PK model using Phoenix, which may be useful in predicting the PK of irinotecan and SN-38 during therapeutic drug monitoring or for establishing PK/PD relationships of irinotecan during inflammation.

CRediT authorship contribution statement

Pavan Kumar Chityala: Conceptualization, Data curation, Formal analysis, Investigation, Methodology, Software, Writing - original draft, Writing - review & editing. **Lei Wu:** Data curation, Formal analysis, Investigation, Methodology, Software, Writing - original draft. **Diana S-L Chow:** Conceptualization, Project administration, Software, Supervision. **Romi Ghose:** Conceptualization, Formal analysis, Funding acquisition, Project administration, Resources, Supervision, Writing - original draft, Writing - review & editing.

Declaration of competing interest

The authors declare that they have no known competing financial interests or personal relationships that could have appeared to influence the work reported in this paper.

References

[1] C. Atasilp, et al., Determination of irinotecan, SN-38 and SN-38 glucuronide using HPLC/MS/MS: application in a clinical pharmacokinetic and personalized medicine in colorectal cancer patients, J. Clin. Lab. Anal. 32 (2018) 3–6.
[2] C. Tian, et al., Value of plasma SN-38 levels and DPD activity I irinotecan-based individualized chemotherapy for advanced colorectal cancer with heterozygous type UGT1A1*6 or UGT1A1*, Cancer Manag. Res. 10 (2018) 6217–6226.
[3] R.H.J. Mathijssen, et al., Clinical pharmacokinetics and metabolism of irinotecan (CPT-11), Clin. Cancer Res. 7 (2001) 2182–2194.
[4] A. Manzanares, et al., Tissue compatibility of SN-38-Loaded anticancer nanofiber matrices, Adv. Healthc. Mater. 7 (2018) 1–11.
[5] C.M. Heske, et al., STA-8666, a novel HSP90 inhibitor/SN-38 drug conjugate, causes complete tumor regression in preclinical mouse models of pediatric sarcoma, Oncotarget 7 (2016).
[6] Q. Zhuang, X. Liu, Z. Sun, H. Wang, J. Jiang, A validated UPLC-MS/MS method to determine free and total irinotecan and its two metabolites in human plasma after intravenous administration of irinotecan hydrochloride liposome injection, J. Pharm. Biomed. Anal. 170 (2019) 112–123.
[7] R. Coriat, et al., Pharmacokinetics and safety of DTS-108, a human oligopeptide bound to SN-38 with an esterase-sensitive cross-linker in patients with advanced malignancies: A phase I study, Int. J. Nanomed. 11 (2016) 6207–6216.
[8] Y. Kawato, M. Aonuma, Y. Hirota, H. Kuga, K. Sato, Intracellular roles of SN-38, a metabolite of the camptothecin derivative CPT-11, in the antitumor effect of CPT-11, Cancer Res. 51 (1991) 4187–4191.
[9] S. Basili, S. Moro, Novel camptothecin derivatives as topoisomerase I inhibitors, Expert Opin. Ther. Pat. 19 (2009) 555–574.
[10] R. Xie, R.H.J. Mathijssen, A. Sparreboom, J. Verweij, M.O. Karlsson, Clinical pharmacokinetics of irinotecan and its metabolites: a population analysis, J. Clin. Oncol. 20 (2002) 3293–3301.
[11] M. Roberts, B. Magnusson, F. Burczynski, M. Weiss, Enterohepatic circulation: physiological, pharmacokinetic and clinical implications, Clin. Pharmacokinet. 41 (2002) 751–790.
[12] P. Riera, et al., Relevance of CYP3A4*20, UGT1A1*37 and UGT1A1*28 variants in irinotecan-induced severe toxicity, Br. J. Clin. Pharmacol. 84 (2018) 1389–1392.
[13] M.-C. Haaz, L. Rivory, R. Christian, L. Vernillet, J. Robert, Metabolism of irinotecan (CPT-11) by human hepatic microsomes: participation of cytochrome P-450 3A and drug interactions, Cancer Res. 58 (1998) 468–472.
[14] M.-C. Haaz, R. Christian, L. Rivory, J. Robert, Biosynthesis of an aminopiperidino metabolite of irinotecan [7-Ethyl-10-[4-(1-Piperidino)-1-Piperidino]Carbonyloxycamptothecine] by human hepatic microsomes, Drug Metab. Dispos. 26 (1998) 769–775.
[15] M.K. Ma, et al., Pharmacokinetics of irinotecan and its metabolites SN-38 and APC in children with recurrent solid tumors after protracted pharmacokinetics of irinotecan and its metabolites SN-38 and APC in children with recurrent solid tumors after protracted low-dose Ir, Clin. Cancer Res. 6 (2000) 813–819.
[16] R. Xie, R.H.J. Mathijssen, A. Sparreboom, J. Verweij, M.O. Karlsson, Clinical pharmacokinetics of irinotecan and its metabolites in relation with diarrhea, Clin. Pharmacol. Ther. 72 (2002) 265–275.
[17] Yasutsuna Sasaki, et al., A Pharmacokinetic and Pharmacodynamic Analysis of CPT-11 and its Active Metabolite SN-38, (1995), pp. 101–110.
[18] M. de Forni, et al., Phase I and pharmacokinetic study of the camptothecin derivative irinotecan, adminstered on a weekly schedule in cancer patients, Cancer Res. 54 (1994) 4347–4354.
[19] A. Eiji, et al., Relationship between Development of Diarrhea and the Concentration of SN-38, an Active Metabolite of CPT-11, (1993), pp. 697–702.
[20] F.A. De Jong, et al., Irinotecan-induced diarrhea: functional significance of the polymorphic ABCC2 transporter protein, Clin. Pharmacol. Ther. 81 (2007) 42–49.
[21] K.W. Cheng, et al., Pharmacological inhibition of bacterial β-glucuronidase prevents irinotecan-induced diarrhea without impairing its antitumor efficacy in vivo, Pharmacol. Res. 139 (2019) 41–49.
[23] A.N. Chamseddine, et al., Intestinal bacterial β-glucuronidase as a possible predictive biomarker of irinotecan-induced diarrhea severity, Pharmacol. Ther. (2019), https://doi.org/10.1016/j.pharmthera.2019.03.002.
[24] R. Ghose, D. White, T. Guo, J. Vallejo, S.J. Karpen, Regulation of hepatic drug-metabolizing enzyme genes by Toll-like receptor 4 signaling is independent of Toll-interleukin 1 receptor domain-containing adaptor protein, Drug Metab. Dispos. 36 (2008) 95–101.
[25] A.E. Aitken, T.A. Richardson, E.T. Morgan, Regulation of drug-metabolizing enzymes and transporters in inflammation, Annu. Rev. Pharmacol. Toxicol. 46 (2006) 123–149.
[26] A.M. Cressman, V. Petrovic, M. Piquette-Miller, Inflammation-mediated changes in drug transporter expression/activity: implications for therapeutic drug response, Expert Rev. Clin. Pharmacol. 5 (2012) 69–89.
[27] E.T. Morgan, Impact of infectious and inflammatory disease on cytochrome P450 –

mediated drug metabolism and pharmacokinetics, Nature 85 (2009) 434–438.
[28] V. Petrovic, S. Teng, M. Piquette-Miller, Regulation of drug transporters: during infection and inflammation, Mol. Interv. 7 (2007) 99–111.
[29] A.E. Aitken, E.T. Morgan, Gene-specific effects of inflammatory cytokines on cytochrome P4502C, 2B6 and 3A4 mRNA levels in human hepatocytes, Ratio 35 (2007) 1687–1693.
[30] R. Ghose, T. Guo, N. Haque, Regulation of gene expression of hepatic drug metabolizing enzymes and transporters by the Toll-like receptor 2 ligand, lipoteichoic acid, Arch. Biochem. Biophys. 481 (2009) 123–130.
[31] A. Gandhi, R. Ghose, Altered Drug Metabolism and Transport in Pathophysiological Conditions vol. 2, (2010).
[32] Z. Mao, et al., Lipopolysaccharide down-regulates carbolesterases 1 and 2 and reduces hydrolysis activity in vitro and in vivo via p38MAPK-NF-κB pathway, Toxicol. Lett. 201 (2011) 213–220.
[33] T.A. Richardson, M. Sherman, D. Kalman, E.T. Morgan, Expression of UDP-glucuronosyltransferase isoform mRNAs during inflammation and infection in mouse liver and kidney, Drug Metab. Dispos. 34 (2006) 351–353.
[36] P. Mallick, P. Shah, A. Gandhi, R. Ghose, Impact of obesity on accumulation of the toxic irinotecan metabolite, SN-38, in mice, Life Sci. 139 (2015) 132–138.
[37] R. Donald Harvey, E.T. Morgan, Cancer, inflammation, and therapy: effects on cytochrome P450-mediated drug metabolism and implications for novel immunotherapeutic agents, Clin. Pharmacol. Ther. 96 (2014) 449–457.
[38] R. Jover, R. Bort, M.J. Gómez-Lechón, J.V. Castell, Down-regulation of human CYP3A4 by the inflammatory signal interleukin-6: molecular mechanism and transcription factors involved, FASEB J. 16 (2002) 1799–1801.
[39] T. Li-Masters, E.T. Morgan, Down-regulation of phenobarbital-induced cytochrome P4502B mRNAs and proteins by endotoxin in mice: independence from nitric oxide production by inducible nitric oxide synthase, Biochem. Pharmacol. 64 (2002) 1703–1711.
[40] C. Fang, et al., Hepatic expression of multiple acute phase proteins and down-regulation of nuclear receptors after acute endotoxin exposure, Biochem. Pharmacol. 67 (2004) 1389–1397.
[41] G.R. Robertson, C. Liddle, S.J. Clarke, Inflammation and altered drug clearance in cancer: transcriptional repression of a human CYP3A4 transgene in tumor-bearing mice, Clin. Pharmacol. Ther. 83 (2008) 894–897.
[42] N.J. Cherrington, A.L. Slitt, N. Li, C.D. Klaassen, Lipopolysaccharide-mediated regulation of hepatic transporter mRNA levels in rats, Drug Metab. Dispos. 32 (2004) 734–741.
[43] K.W. Renton, Alteration of drug biotransformation and elimination during infection and inflammation, Pharmacol. Ther. 92 (2001) 147–163.
[44] K.W. Renton, Cytochrome p450 regulation and drug biotransformation during inflammation and infection, Curr. Drug Metab. 5 (2004) 235–243.
[45] E.T. Morgan, Regulation of cytochrome P450 by inflammatory mediators: why and how? Drug Metab. Dispos. 29 (2001) 207–212.
[46] E.T. Morgan, et al., Symposium report regulation of drug-metabolizing enzymes and transporters in infection, inflammation, and cancer, Pharmacology 36 (2008) 205–216.
[47] M.A. Panaro, et al., Expression of UDP-glucuronosyltransferase 1A6 isoform in Caco-2 cells stimulated with lipopolysaccharide, Innate Immun. 16 (2009) 302–309.
[48] X. Zhou, et al., Disturbance of hepatic and intestinal UDP-glucuronosyltransferase in rats with trinitrobenzene sulfonic acid-induced colitis, Drug Metab. Pharmacokinet. (DMPK) 450 (2012) 1–31 2.
[49] D. Yao, Q. Dong, Y. Tian, C. Dai, S. Wu, Lipopolysaccharide stimulates endogenous β-glucuronidase via PKC/NF-κB/c-myc signaling cascade: a possible factor in hepatolithiasis formation, Mol. Cell. Biochem. 444 (2018) 93–102.
[50] C.J. Van Groeningen, et al., Altered pharmacokinetics and metabolism of CPT-11 in liver dysfunction: a need for guidelines, Clin. Cancer Res. 6 (2000) 1342–1346.
[51] E. Rouits, S. Guichard, P. Canal, E. Chatelut, Non-linear pharmacokinetics of irinotecan in mice, Anti Canccer Drugs 13 (2002) 631–635.
[52] R. Xie, R.H.J. Mathijssen, A. Sparreboom, J. Verweij, M.O. Karlsson, Clinical pharmacokinetics of irinotecan and its metabolites in relation with diarrhea, Clin. Pharmacol. Ther. 72 (2002) 265–275.
[53] C.E. Klein, et al., Population pharmacokinetic model for irinotecan and two of its metabolites, SN-38 and SN-38 glucuronide, Clin. Pharmacol. Ther. (2002), https://doi.org/10.1067/mcp.2002.129502.